Frequency and power of human alpha oscillations drift systematically and independently with time-on-task

Christopher S.Y. Benwell[1*], Raquel E. London[2], Chiara F. Tagliabue[3], Domenica Veniero[1], Joachim Gross[1,4], Christian Keitel[1*], Gregor Thut[1*]

[1] Centre for Cognitive Neuroimaging, Institute of Neuroscience and Psychology, University of Glasgow, Glasgow, UK

[2] Department of Experimental Psychology, Ghent University, 9000 Ghent, Belgium

[3] CIMEC – Center for Mind/Brain Sciences, Università degli Studi di Trento, Trento, Italy

[4] Institut für Biomagnetismus und Biosignalanalyse, Westfälische Wilhelms-Universität, Malmedyweg 15, 48149 Münster, Germany

* These authors have contributed equally

Corresponding author: Christopher S.Y. Benwell

Institute of Neuroscience and Psychology, 58 Hillhead Street, Glasgow, UK. G12 8QB

Christopher.Benwell@Glasgow.ac.uk

Running title: Systematic non-stationarities in human alpha oscillations

Keywords: alpha; neural oscillation; EEG; non-stationarity; frequency sliding

Abstract

Oscillatory neural activity is a fundamental characteristic of the mammalian brain spanning multiple levels of spatial and temporal scales. Current theories of neural oscillations and analysis techniques employed to investigate their functional significance are based on an often implicit assumption: In the absence of experimental manipulation, the spectral content of any given EEG- or MEG-recorded neural oscillator remains approximately stationary over the course of a typical experimental session (~1 hour). Here, we show that this assumption is inaccurate for ongoing neural oscillations in one of the most prominent frequency bands of the EEG/MEG signal, the alpha band (8:13 Hz). We found that alpha peak frequency systematically decreased over time, while alpha power increased. Intriguingly, these systematic trends occurred independently of each other suggesting the existence of two non-stationary endogenous processes inherent in macroscopic alpha band activity. Our findings provide novel insight into the time-varying intrinsic properties of large-scale neural networks. They have important implications for the analysis and interpretation of studies that aim at identifying functionally relevant oscillatory networks or at driving them through external stimulation.

Significance statement

Mounting evidence suggests that neural oscillations underlie cognitive processes in the brain. Hence, mapping endogenous characteristics of oscillatory networks represents an important venture for modern neuroscience. Here, we reveal two endogenous non-stationary processes occurring in the alpha band - a prominent rhythm of the brain. Alpha peak frequency systematically decreased and alpha power systematically increased over ~1 hour of

psychophysical task performance, even during trial baselines. These non-stationarities do not appear to be two manifestations of a single process but rather two independent effects. These findings inform signal processing and neuro-stimulation techniques and advance our understanding of the physiology of functionally relevant neural oscillations.

Introduction

Rhythmic neural activity is ubiquitous across multiple spatial scales of the nervous system and across species (1). Since the invention of electroencephalography (EEG; see 2), reliable associations have been revealed between distinct cognitive states/functions and frequency-specific EEG activity in humans (3, 4). This has led to various proposals that oscillatory activity may represent a fundamental computational mechanism underlying information encoding and transfer between distinct brain regions and across temporal scales (5-11).

Oscillatory alpha-band (~8-13 Hz) activity represents one of the most prominent features of the EEG in the waking brain. A substantial body of evidence links this activity to processes such as perception (12-16), attention (17-19) and memory (20-23). More specifically, alpha power is inversely related to cortical excitability (24-26), and an increase in alpha power has been linked to the functional inhibition of cortical regions responsive to information that is irrelevant for the task at hand (27, 28), potentially by gating the communication from local neural activity to other cortical regions (10, 29). However, neural oscillations as recorded with EEG or MEG (M/EEG) can reflect a large mixture of generating processes in terms of both local micro-circuitry and large-scale networks. For instance, recent animal studies have revealed multiple distinct alpha generators with different functional and/or laminar profiles (30-35). Hence, while oscillatory activity within one frequency band measured at the macroscale is

typically interpreted as a single process within a unitary framework (e.g. alpha for gating), this assumption is likely an over-simplification (36). An accurate theory of the functional relevance of alpha (and other) rhythms at the macroscale therefore needs to account for characteristics of neural dynamics that are often missed and/or ignored by standard approaches to spectral analyses.

Most M/EEG experiments employ designs and analyses that are based on a variety of implicit assumptions regarding the characteristics of the activity of interest (for an overview see 37). Yet, neural time series frequently violate a number of these assumptions. For instance, recent work suggests that typical M/EEG spectral analysis techniques may mask non-sinusoidal oscillatory characteristics of potential functional relevance (38-41). Moreover, these analysis approaches as well as common experimental designs assume approximate stationarity (both short and long term) of the spectral characteristics of the underlying neural oscillator(s). In the absence of experimental manipulation, neural oscillators are assumed to show only weak spontaneous fluctuations around their mean frequency and power, leading in the case of alpha activity to the characteristic, band-limited alpha peak in the power spectrum. However, across the course of an experimental session, tonic power changes in certain frequencies (such as an increase in alpha-band power) (42-44) and state- and stimulus-dependent fluctuations in oscillation peak frequency have been reported (45), even during two minute resting-state EEG recordings (46, for an overview see 47). These non-stationarities of oscillatory activity are of potential theoretical importance but rarely accounted for when analysing experimental data.

Here, we re-analysed two previously published data sets (see 16, 47) to investigate the degree of non-stationarity of two fundamental oscillatory characteristics – frequency and power – in

the alpha-band over the course of a typical EEG experimental session. Importantly, we found a systematic decrease in individual alpha peak frequency accompanied by a concurrent but independent increase in alpha power. We conclude that these measures capture long-term deterministic non-stationarities inherent to underlying neural alpha generators. This confirms that assuming stationarity of oscillatory activity is invalid in many circumstances and has direct implications for the analysis and interpretation of brain oscillations and their functional relevance.

Results

We analysed combined EEG data from two experiments that were recorded using the same EEG hardware and 60 scalp electrodes, after verifying that analysing each data set on its own revealed the same pattern of results. Both experiments lasted approximately the same amount of time (~1 hour) and had similar trial structures. One of the experiments involved a line bisection task (N=20 participants; see 48) and the other a luminance discrimination task (N=14 participants; see 16). Since our primary aim was to investigate the degree of non-stationarity of ongoing, baseline oscillatory activity (in the absence of stimulus processing) over the course of an experimental session, we combined pre-stimulus epochs (duration = 1 sec) across both datasets in order to increase statistical power (overall N = 34 participants). The two oscillatory measures of interest were the alpha-band power and peak frequency.

Baseline alpha-power and -frequency show non-stationarity over time

In order to investigate changes in power and frequency over time, we initially split trials into the 1st and 2nd half of the experimental session within each participant. Fast Fourier Transforms (FFT) were applied to 1-sec single-trial baseline epochs (1 epoch per trial, see methods) and the resulting power spectra were averaged over all trials in each split-half bin separately (i.e. separately for the 1st and 2nd half of the experiment). This yielded one power spectrum per split-half and per EEG sensor. For each participant, we then extracted peak alpha frequency and peak alpha power values from the sensor with the highest average power within the alpha (8-13Hz) band. Figure 1A plots grand-averaged power spectra centred on the alpha band for the 1st (blue) and 2nd (red) half of the experimental session respectively. The peak frequency values are denoted by the vertical dashed lines. This plot suggests that over time peak alpha frequency *decreased*, whereas alpha power *increased*.

Figures 1B and C plot for each participant the change in individual alpha frequency (IAF) and power over time (2nd half IAF minus 1st half IAF), highlighting the consistency of the effects across participants for both measures. The group median IAF was 10.35 Hz for the 1st half of the experimental session (standard deviation = 0.89 Hz, range: 8.4-11.7 Hz) and 10.1 Hz for the 2nd half (standard deviation = 0.9 Hz, range: 8.2-11.4 Hz). Although the frequency shift was small on average (0.25Hz), shifts within individuals could reach 2Hz (see Fig 1B). Paired-sample t-tests confirmed a group-level reduction in IAF ($t(33) = -2.5755$, $p = .0147$, Cohen's $d = .442$) and an increase in alpha-power over time ($t(33) = 3.35$, $p = .002$, Cohen's $d = .823$). However, the individual changes in peak alpha frequency did not correlate with the individual changes in alpha power across participants (Spearman's Rho = -0.038, $p = .8305$). Figure 1D plots grand-averaged topographies of alpha-power (8-13 Hz) for the 1st (top) and 2nd (bottom)

half of the experimental session respectively, revealing similar spatial distributions but an increase in amplitude over time.

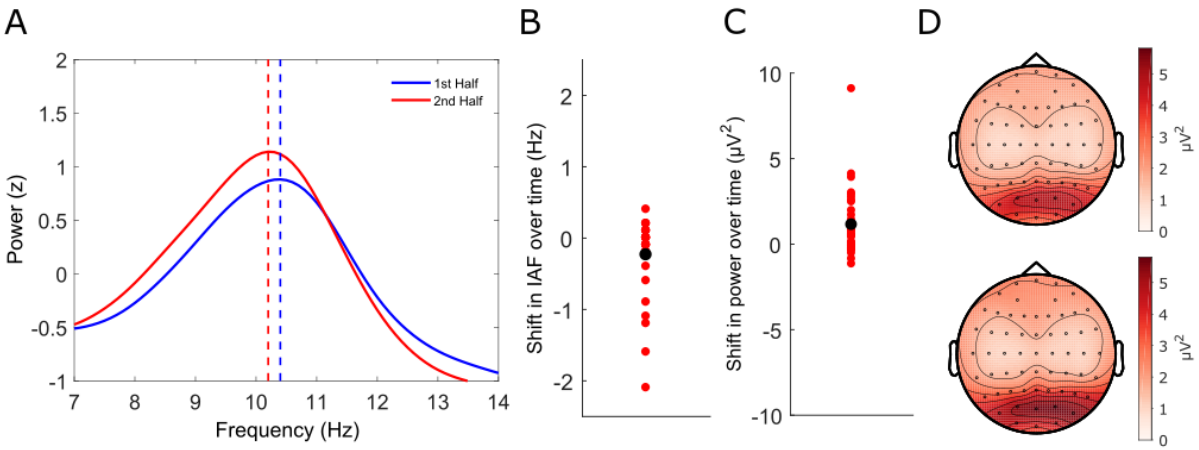

Figure 1: Split-half Fast Fourier Transform (FFT) analysis. **(A)** Grand-averaged frequency spectra (z-scored) in the alpha band from trial baselines for both the 1st (solid blue line) and 2nd (solid red line) halves of the experimental session. The peak frequency values are denoted by vertical dashed lines (blue = 1st half, red = 2nd half). Alpha power increased whereas peak alpha frequency decreased from the 1st to the 2nd half of the experimental session. **(B)** Shifts in individual alpha frequency from the 1st to the 2nd half of the experimental session. Red dots denote individual participants and the black dot represents the group average shift. **(C)** Shifts in individual alpha power from the 1st to the 2nd half of the experimental session. Red dots denote individual participants and the black dot represents the group average power change. **(D)** Grand-averaged topographies of alpha power (8-13 Hz) for the 1st (top) and 2nd (bottom) half of the experimental session respectively. The topographical distributions were almost identical but the increase in amplitude over time is apparent.

Comparing frequency-power relationship between shorter and longer time scales

Recently, Cohen (46) introduced a new approach allowing for the calculation of time-resolved frequency content, the instantaneous frequency, in M/EEG signals. Note that the instantaneous frequency is defined as the change in the phase of an oscillator per unit time (see materials and methods section for details, instantaneous alpha frequency calculation adopted from 46). Cohen found a non-linear (inverted u-shape) relationship between estimates of instantaneous alpha frequency (Inst-AF) and band-limited alpha power in two

minute resting-state EEG recordings. Here, we replicated this finding with time-resolved data from the single-trial baseline alpha activity from which we determined alpha power and Inst-AF. Both measures were averaged within consecutive 20 ms segments for each 1-sec baseline epoch, electrode and participant separately to preserve variability on the short time scale (i.e. within trials) and then z-scored within participants. Alpha-power was then plotted against Inst-AF (see Fig 2A for a representative sample of participants, and Fig 2B for the group average). A consistent relationship between alpha power and alpha frequency across time-points of the 1-sec epoch (i.e. on a short time scale) is revealed, with increased variability and higher maximum power values close to the central alpha frequency. The inverted u-shaped relationship was formally tested using the two-line solution proposed by Simonsohn (49). This method involved performing linear regression between Inst-AF and power separately for 'high' (in our case, z-values above 0) and 'low' (z-values below zero) values of the independent variable (Inst-AF values) for each participant. If a significant inverted u-shaped relationship exists, then the coefficients for the 'high' and 'low' regressions should be opposite in sign and both individually statistically significant. The analysis revealed a significant positive relationship between low (below 0) z-values of Inst-AF and power (t-test of coefficients across group against 0: $t(33) = 8.7979$, $p < .0001$) and a significant negative relationship between high (above 0) z-values of Inst-AF and power ($t(33) = -18.8715$, $p < .0001$), thereby formally confirming the inverted u-shaped relationship between time-resolved Inst-AF and power.

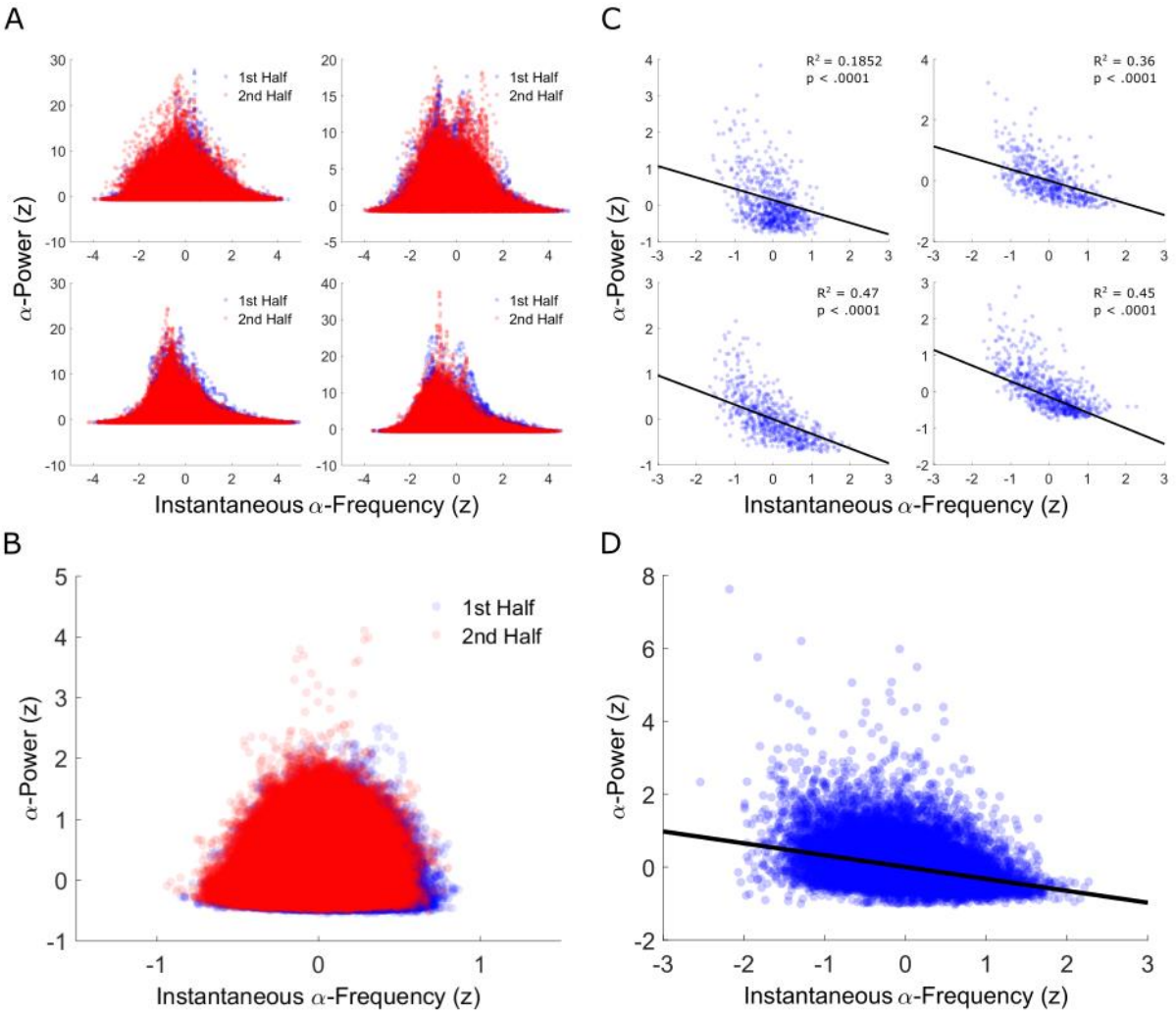

Figure 2: Comparing the alpha frequency-power relationship between shorter and longer time scales **(A)** Scatterplots of short time-scale resolved (20 ms resolution from all single trial baselines) instantaneous alpha frequency (x-axis: z-scored) versus alpha power (y-axis: z-scored) values from the 1st (blue dots) and 2nd (red dots) halves of the experimental session from four representative participants. Note that data are included from all electrodes and single-trial time-points for these four participants. **(B)** Group-averaged scatterplot of short time-scale resolved instantaneous alpha frequency (x-axis: mean z-scores) versus alpha power (y-axis: mean z-scores) values from the 1st (blue dots) and 2nd (red dots) halves of the experimental session. Note that the number of trials included was limited to the first 490 (245 in each bin) in order to be able to average over participants. Both **A** and **B** show systematic frequency-power variability with increased variability and higher amplitude of power values close to the central alpha frequency (replicating 45). **(C)** Scatterplots of longer time-scale resolved (averaged over time-points within each single trial baseline) instantaneous alpha frequency (x-axis: z-scored) versus alpha power (y-axis: z-scored) values from the same 4 participants as in **A**. **(D)** Group-averaged scatterplot of longer time-scale resolved instantaneous alpha frequency (x-axis: z-scored) versus alpha power (y-axis: z-scored) values. Both **C** and **D** show that emphasising the longer-term time-scale (across trials) highlights an inverse relationship between instantaneous alpha frequency and alpha power in addition to the parabolic relationship observed at the short-term scale (within trials).

However, our split-half data binning analyses above suggest that both measures also change systematically over a longer time-scale (i.e. across trials over the course of an experiment), with alpha frequency decreasing and power increasing. Hence, we re-represented the data as frequency-power distributions after averaging Inst-AF and power values over each 1-sec baseline epoch per electrode to emphasize the variability across a longer time scale (i.e. across trials) and performed regression analysis between these values. Figure 2C-D shows the corresponding scatter plots of Inst-AF values (x-axis) versus power values (y-axis) for the same representative participants as in Figure 2A (see Fig 2C), along with the group average (see Fig 2D). We tested for both monotonic and nonlinear relationships between baseline-averaged Inst-AF and power and found a significant negative overall linear relationship ($t(33) = -4.1123$, $p < .0001$) but no inverted u-shaped relationship as the Inst-AF-power regression for both the low and high Inst-AF bins showed significant negative relationships (low Inst-AF values versus power: $t(33) = -2.1746$, $p = .0369$, high Inst-AF values versus power: $t(33) = -6.6183$, $p < .0001$). This confirms that introducing a longer-term time scale (across trials) results in an inverse relationship between Inst-AF and power, as opposed to the parabolic relationship observed at the short-term scale (within trials).

Frequency sliding and power increase confirmed with time-resolved analysis of instantaneous frequency and power

Next, we performed a time resolved analysis across 2-sec single-trial, stimulus-locked epochs spanning both baseline and post-stimulus periods (-1 to +1 sec from stimulus-onset). Post-stimulus data were included to test whether the relationships held for both pre- and post-stimulus periods. For each participant, we calculated estimates of alpha power (8:13 Hz) and

Inst-AF over each epoch (with 20ms resolution as before). We then performed within-participant, single-trial Spearman's correlations between trial order (1:*N trials*) and both single-trial alpha-power and Inst-AF separately at each time-point across the epoch. Figure 3 displays the results of group-analyses in which we investigated whether correlation coefficients differed from zero systematically (i.e. negative or positive) across participants using one-sample t-tests at each time point and cluster-corrected analysis (50). In line with the split-half analyses, the results revealed that Inst-AF was negatively correlated with trial-order (Figure 3A, systematic decrease over the course of the experimental session), whereas alpha-power was positively correlated with trial-order (Figure 3D, systematic increase over the course of the experimental session). Both effects spanned the entire epoch (Figure 3A, 3D). Their respective pre-stimulus topographic representations (averaged over -1 to -0.5 sec to avoid the possible inclusion of post-stimulus activity) are shown in Figure 3B and 3E. Figure 3C shows the relationship between trial number (x-axis) and z-scored single-trial Inst-AF (averaged over -1:-0.5 sec across all electrodes in each single-trial baseline period; y-axis) collapsed across all participants. The black line represents the best-fitting regression slope. On average, the alpha peak frequency decelerated by 0.2 Hz per hour. A Spearman's correlation applied to this collapsed data confirmed a highly significant negative relationship (rho = -0.1131, p<.0001). Figure 3F shows the relationship between trial number and z-scored single-trial alpha-power. A highly significant positive relationship was confirmed (Spearman's Rho = 0.1222, p<.0001).

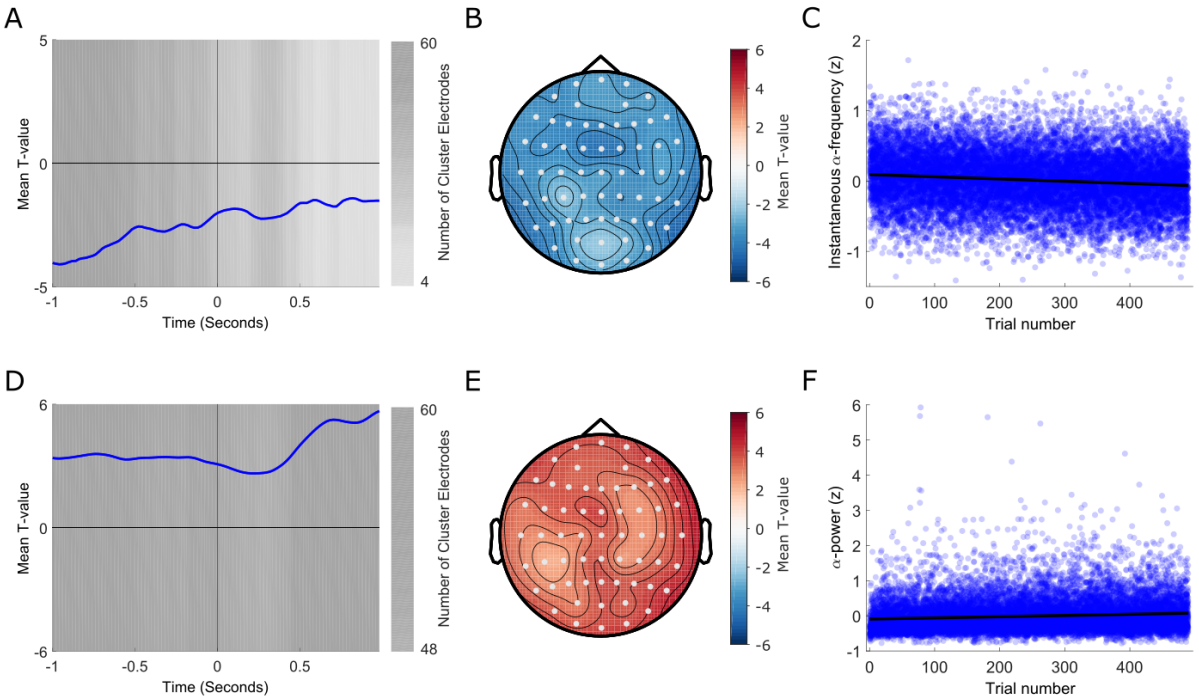

Figure 3: Time-resolved analysis of frequency sliding and power changes. **(A)** Trial order-instantaneous alpha frequency effect: T-values averaged over all electrodes. A negative t-value indicates a decrease in frequency over trials. Significant time-points are indexed by the grey background fill. One significant negative cluster was found which spanned the entire epoch. Hence, this analysis confirmed that alpha-frequency systematically decreased over the course of the experimental session at both pre- and post-stimulus time points. The luminance of the background fill indicates how many electrodes were included in the significant cluster at each time-point (the darker the fill, the more electrodes are included in the cluster at this time-point). **(B)** Topographic representation of the t-values averaged over the pre-stimulus (-1:-0.5 sec) portion of the significant cluster. Electrodes that were included in the cluster at least once at any time-point during this time period are highlighted in white. **(C)** Scatterplot of the relationship between trial number (x-axis) and instantaneous alpha frequency (y-axis: z-scored and averaged over -1:-0.5 sec across all electrodes in each single-trial baseline period). Note that the data for all participants are included and the number of trials included was again limited to the first 490 to equalise across participants. The solid black line represents the best-fitting regression slope. **(D)** Trial order to alpha power effect: T-values values averaged over all electrodes. A positive t-value indicates an increase in power over trials. Significant time-points are indexed by the grey background fill. One significant positive cluster was found which spanned the entire epoch. Hence, this analysis confirmed that alpha power systematically increased over the course of the experimental session at both pre- and post-stimulus time points. The luminance of the background fill indicates how many electrodes were included in the significant cluster at each time-point (the darker the fill, the more electrodes are included in the cluster at this time-point). **(E)** Topographic representation of the t-values averaged over the pre-stimulus (-1:-0.5 sec) portion of the significant cluster. Electrodes that were included in the cluster at least once at any time-point during this time period are highlighted in white. **(F)** Scatterplot of the relationship between trial number (x-axis) and alpha power (y-axis: z-scored and averaged over -1:-0.5 sec across all electrodes in each single-trial baseline period). Note that the data for all participants are included and the number of trials included was again limited to the first 490 to equalise across participants. The solid black line represents the best-fitting regression slope.

Frequency sliding and power increases in the alpha-band over time are driven by partially independent processes

We then investigated to what extent the decrease in alpha frequency and increase in alpha power over time are linked by employing a stratification analysis. We hypothesised that if the frequency decrease and power increase are manifestations of the same process, holding constant the value of one measure between the 1st and 2nd half of the experiment should also abolish the change in the other measure. For example, if the Inst-AF decrease over time is co-varying exactly with the increase in power, then when power is held constant the Inst-AF should also remain stationary (and vice versa). To test this, we calculated single-trial values of both baseline alpha power (8:13 Hz) and Inst-AF (averaged over -1:-0 sec) and split the single-trial data into bins corresponding to the 1st and 2nd half of the experiment in each participant. We then approximately equalised the mean, variance and all higher order statistics of the distributions within each bin for one of the measures (power or Inst-AF) by sub-sampling the single-trials (see Materials and methods for details). After stratification in one dimension (either alpha power or Inst-AF), FFT analysis was then applied to 1-sec baselines to obtain peak alpha frequency and peak alpha amplitude from averaged frequency spectra of the stratified trials in the 1st- and 2nd-half bins separately.

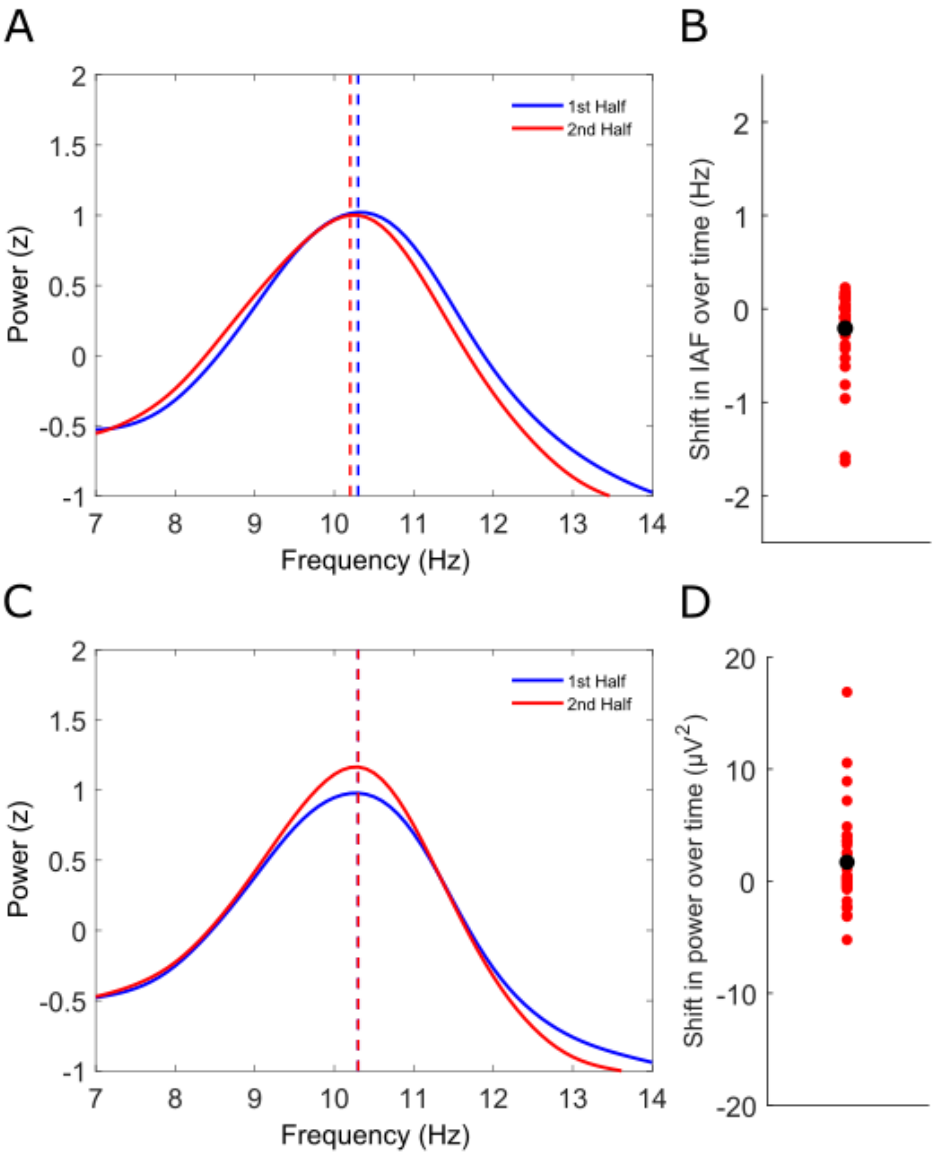

Figure 4: Trial stratification analysis reveals non-stationary processes are at least partially independent. **(A)** Analysis with power held approximately constant between the 1st and 2nd half of the experiment through trial sub-sampling: Grand-averaged frequency spectra (z-scored) in the alpha band from stratified trial baselines for both the 1st (solid blue line) and 2nd (solid red line) halves of the experimental session. The peak frequency values are denoted by vertical dashed lines (blue = 1st half, red = 2nd half). Despite alpha power remaining approximately stationary, peak alpha frequency still decreased from the 1st to the 2nd half of the experimental session. **(B)** Shifts in individual alpha frequency (IAF) from the 1st to the 2nd half of the experimental session from the power stratification analysis. Red dots denote individual participants and the black dot represents the group average shift. **(C)** Analysis with instantaneous frequency held approximately constant between the 1st and 2nd half of the experiment through trial sub-sampling: Grand-averaged frequency spectra (z-scored) in the alpha band from stratified trial baselines for both the 1st (solid blue line) and 2nd (solid red line) halves of the experimental session. The peak frequency values are denoted by vertical dashed lines (blue = 1st half, red = 2nd half). Despite alpha frequency remaining approximately stationary, alpha power still increased from the 1st to the 2nd half of the experimental session. **(D)** Shifts in individual alpha power from the 1st to the 2nd half of the experimental session from the instantaneous frequency stratification analysis. Red dots denote individual participants and the black dot represents the group average power change.

Figures 4A-B plot the results of the power stratification analysis (i.e. when power was held constant between the 1st and 2nd split-half bins of the experiment). Despite power being held constant, the grand average peak alpha frequency still decreased from the 1st to the 2nd half of the experiment (Figure 4A) as denoted by the vertical dashed lines (blue = 1st half, red = 2nd half). Figure 4B plots the change in peak alpha frequency over time (2nd half IAF minus 1st half IAF) for each participant. A paired t-test confirmed a group-level reduction in peak alpha frequency ($t(33) = -2.8497$, $p = .0075$). Figures 4C-D plot the results of the Inst-AF stratification analysis (i.e. when Inst-AF was held constant between the 1st and 2nd split-half bins of the experiment). Again, despite Inst-AF being held constant, alpha power increased from the 1st to the 2nd half of the experiment (Figure 4C). Figure 4D plots the change in alpha power over time for each participant, which also remained significant ($t(33) = 2.1759$, $p =.0368$). Hence, when power was held constant, the decrease in peak alpha frequency overtime was maintained and when Inst-AF was held constant, the increase in power over time was also maintained. Overall, this suggests that frequency sliding and power changes over time are not likely to be two manifestations of the same process but rather may index two partially independent non-stationary processes in the alpha-frequency band.

Discussion

The results of the current study highlight the existence of two endogenous non-stationary processes in human alpha-band EEG activity. Over the course of an experimental session (~1 hour), peak alpha-frequency decreased whereas alpha-power increased, even in the absence of external stimulation (i.e. during trial baselines). Furthermore, the frequency decrease and power increase were partially independent and hence do not appear to be two manifestations

of the same process. These findings have several important theoretical, methodological and applied implications, as they call into question fundamental assumptions underlying current theories and approaches in both electrophysiological research and oscillatory brain stimulation techniques at the macro-scale.

Implications for understanding neural network activity at the macro-scale

Over the past two decades, evidence has converged on a more dynamic functional role of alpha oscillations in sensation and cognition than previously thought (51). Currently, alpha oscillations are considered to be implicated in the orchestration of active inhibition vs. facilitation of task-irrelevant vs. task-relevant brain regions (19, 27, 52) and the interregional gating or communication of information (10, 28, 29, 53). The current study highlights the existence of systematic non-stationarities in alpha band limited power density and frequency structure. The systematic increase in alpha power over time replicates previous studies, which have associated the effect with the level of sustained attention and fatigue (42-44, 54-56). Such slow drifts in EEG power over the course of an experimental session have also been found to relate to non-stationarities in psychophysical performance (48, 57, 58). In terms of alpha frequency, previous studies have shown both long-term changes related to aging and pathology (20, 47, 59) and short-term changes related to sensory stimulation and cognitive engagement. For instance, alpha frequency has been shown to increase in response to sensory stimulation and task engagement, particularly under conditions of high stimulus intensity and/or cognitive demand (45, 46, 60-62). Endogenous alpha frequency fluctuations have also been observed in resting state EEG (46). These findings, along with computational modelling approaches, have led to proposals that frequency shifts may represent a general

mechanism of multiscale interactions in the brain, controlling neuronal spike timing and coordinating large-scale neural network activity (47).

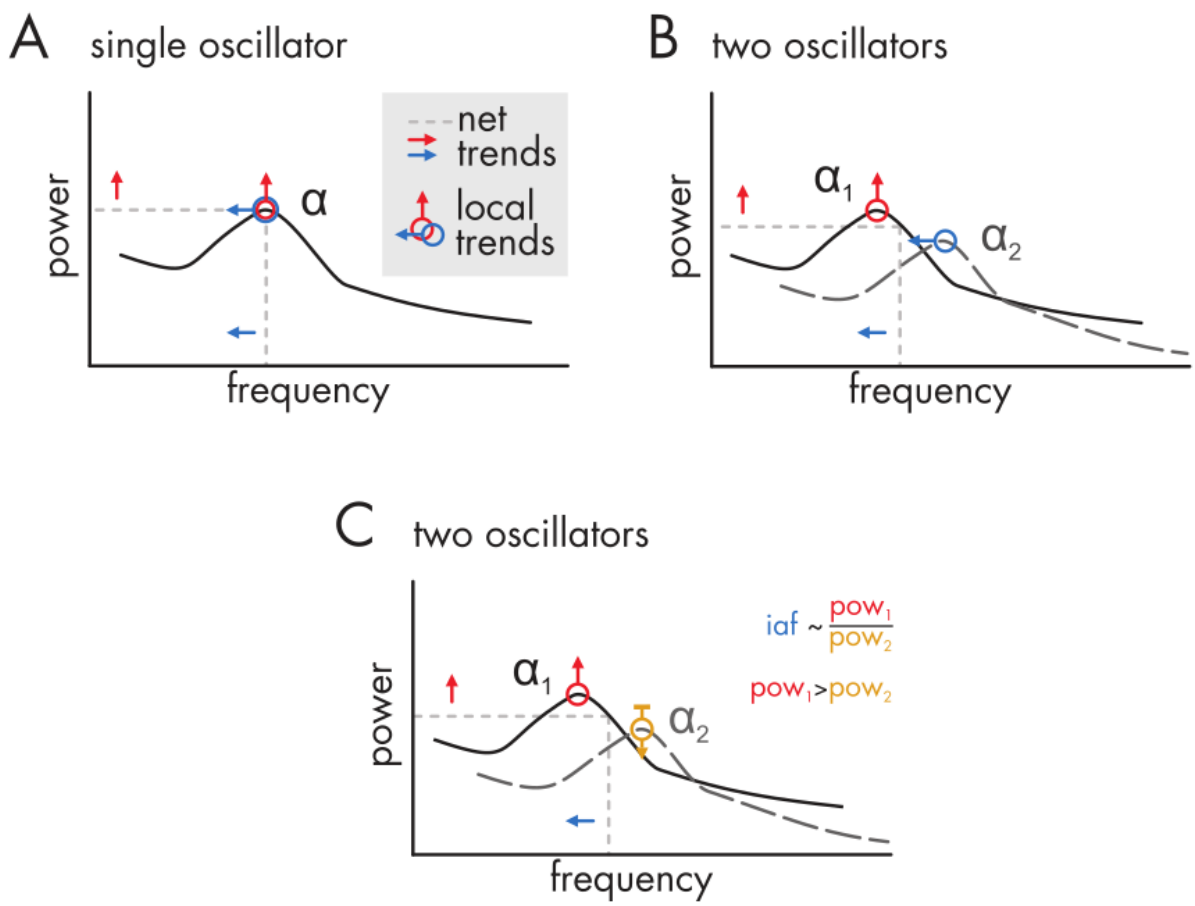

Figure 5: Three candidate scenarios underlying systematic long-term alpha frequency decrease and alpha power increase (= net trend). Black lines (straight and dashed in **B** and **C**) depict schematic power spectra of underlying neural assemblies oscillating at a mean (peak) alpha frequency (with spontaneous fluctuations around the mean over trials determining peak width). Note that all scenarios produce the same net trends in changes over time (red and blue arrows on grey dashed lines). (**A**) Alpha, as measured with M/EEG, is generated by a single process that increases its power (red arrow) and reduces its frequency (blue arrow) over time. This scenario fits our data only when assuming that both systematic effects stem from independent influences. (**B**) Our findings of independent power and frequency changes may also speak to the presence of (at least) two generative processes that produce alpha rhythms (black straight and dashed lines; for evidence see recent findings in 34, 35). One of them increases in power (e.g. α_1, red arrow), while the other decreases in frequency over time (e.g. α_2, blue arrow). (**C**) Changes in power only (red and golden arrows), of two generative processes with offset peak frequencies (α_1 and α_2), may also explain net trends. Their power ratio can influence the estimate of individual alpha frequency because peaks are not readily separable in EEG data (instead, EEG measurements capture a weighted sum of single spectra). Scenario (**C**) is unlikely as our data show that power and frequency changes are unrelated. Note that these scenarios are necessarily simplifications of a more complex cortical reality that may involve multiple oscillating micro-circuits (38) with non-sinusoidal properties (39-41).

While largely in line with the few previous studies reporting non-stationarities in alpha-power and frequency, our data provide novel insights into their potential sources of origin, albeit at the spatial resolution of macroscale EEG which is inherently limited. The macroscale activity of widespread, larger cell assemblies has been postulated to give rise to slower oscillations and also higher power density than local, smaller cell assemblies (63), and so changes in the extent of the oscillating network engaged over time could explain an increase in power and a concurrent decrease in frequency. We believe that this explanation can be ruled out. If the power increase and frequency decrease were two manifestations of a single process, we would have expected them to correlate systematically, which was not the case. Conversely, the existence of two apparently independent alpha non-stationarities suggests that they may arise from distinct neural sources (see Figure 5 for a series of scenarios which may explain the non-stationarities we observed in our EEG data). Whether this independence originates from two separate influences onto the same alpha generating process (Fig 5A), or rather represents shifts in the characteristics of two individual oscillators over time (Fig 5B), remains an open question. However, our finding of independent power and frequency changes is not in line with a scenario in which the frequency decrease is merely a by-product of a power ratio change between two alpha generating processes (Fig 5C). Therefore, changes in alpha power and frequency seem to reflect two neurophysiologically and potentially also functionally distinct processes.

Recently, neurophysiological studies have begun to shed light on the sources of alpha activity and their relationship with measures of neural activity at different spatial and temporal scales. For instance, alpha power has been shown to be inversely related to both the blood-oxygen-

level dependent (BOLD) signal (33, 64, 65) and cortical excitability as measured by single cell recordings in monkeys (25). However, the functional characteristics of different alpha sources, and their relationships with other neurophysiological measures, appear not to be uniform. They rather seem to depend on their cortical region and/or laminar profile, suggesting multiple processes related to alpha-band activity (30, 32-35, 66-70). In line with this recent work our discovery of two independent power and frequency non-stationarities suggests that alpha activity measured by surface EEG does not reflect a unitary rhythm but rather arises from a mixture of generating mechanisms with potentially different neurophysiological and functional characteristics. Future studies will need to capitalize on analysis techniques that also account for frequency dynamics. This will help to identify sources of distinct non-stationarities and their functional relevance to gain a detailed understanding of alpha oscillations and their role in cognition.

Methodological and applied implications

Systematic endogenous non-stationarity of both the frequency structure and the power density of alpha activity invalidates assumptions underlying some of the most frequently employed M/EEG time-frequency analysis procedures. For instance, in the absence of experimental manipulation, stationarity of oscillatory characteristics is often assumed, or intrinsic (i.e. baseline) fluctuations are interpreted to represent stochastic or spontaneous processes (71, 72). However, band-limited EEG spectral properties can be non-stationary at the sub-second time scale, thereby potentially violating assumptions of the most common methods of spectral analysis such as Fourier and wavelet-based transformation (37, 46, 72). The current study demonstrates that non-stationarities also occur at longer time-scales in the

order of minutes/hours. These long-term non-stationarities of the EEG signal give rise to several important methodological caveats and should be taken into account when designing, analysing and interpreting any experiment involving the identification of M/EEG-behaviour relationships. This is particularly important given that many commonly employed behavioural measures such as psychometric function threshold and slope, detection rate and decision criterion can also be non-stationary over time (48, 58, 73, 74). Crucially, in situations where both the EEG and behavioural measures of interest display non-stationarity, a correlation between the two may be detected simply because both measures systematically change over time (i.e. they both independently correlate with trial order across the experiment). If this possibility is not investigated and/or accounted for then a potentially epiphenomenal correlation between the two measures may be misinterpreted as a causal or functional relationship. Alternatively, some non-stationarities in the EEG signal may represent candidate neural correlates of non-stationary psychophysical performance (57, 58) and so functionally relevant relationships may be missed if they are not accounted for. Hence, it is critical that non-stationarity is considered in order to obtain a more accurate impression of the sources of any observed brain/behaviour relationship.

The current results also have implications for attempts to entrain oscillatory neural activity through exogenous methods such as visual flicker (75-79, but see 80, 81) and non-invasive transcranial brain stimulation (NTBS) (82, 83). On the one hand, the existence of short- and long-term frequency sliding suggests that peak alpha frequency is 'flexible' over time and hence potentially amenable to control through external intervention. Accordingly, recent studies employing NTBS techniques have provided tentative evidence for neurophysiological and/or behavioural changes linked to alpha-frequency tuned stimulation (84, 85), with stimulation inducing behavioural changes even when slightly offset from the peak frequency

(86), which is in line with frequency sliding also being behaviourally relevant (87). On the other hand, it is not exactly clear how to interpret the peak frequency as measured by EEG either biologically or functionally. The heterogeneous nature of the sources of alpha activity contributing to the EEG signal (30, 32-35, 66-69, 70, our data) invalidates the assumption that the peak alpha frequency necessarily represents a single endogenous 'oscillator' and hence raises questions regarding the rationale of targeting a peak frequency for entrainment. Therefore, precise targeting of oscillatory networks by NTBS will benefit from more refined considerations with regard to the frequency and power content of the EEG signal, and their origin and functional roles.

Materials and methods

Participants

Analyses were carried out on the data from 34 individuals (15 males, 19 females, mean age: 24, min = 17, max = 33) who participated in two separate experiments. 20 participated in a line bisection experiment (16) and 14 participated in a luminance discrimination experiment (48). The exact protocols for each experiment are available in the original papers, but every aspect of the designs and analyses that are relevant for the current study are described below. All participants gave written informed consent to participate and were financially compensated for their time. The study was approved by the Ethics Committee of the College of Science and Engineering at the University of Glasgow. The experimental sessions were carried out within the same lab at the Institute of Neuroscience and Psychology at the University of Glasgow.

Instrumentation and stimuli

In both experiments, different visual discrimination tasks were performed but we combined the datasets because we were primarily interested in endogenous changes in the EEG activity during the pre-stimulus trial baselines occurring irrespective of the visual stimulus and the task performed. Full descriptions of the rationale, methodology and results for each experiment are available in the original papers (16, 48) but a brief description of each experimental protocol is provided below.

Experiment 1

Participants performed a computerised line bisection task in which they were asked to estimate which of two segments of a pre-bisected horizontal line was shortest. On any given trial, the line could be 1 of 3 lengths and pre-bisected at 1 of 13 horizontal locations. The stimuli were presented using the E-Prime software package (88) on a CRT monitor with a 1280 x 1024 pixel resolution and 85 Hz refresh rate. Participants were seated 70 cm from the monitor with their midsagittal plane aligned to the centre of the screen and their chin in a chin rest. Each trial began with presentation of a black fixation cross (subtending 0.4° x 0.4° VA) which remained on the screen for 3 s followed by presentation of the pre-bisected line (0.15 s). Following the disappearance of the line, the fixation cross remained on the screen until the participant indicated which end of the line had appeared shortest to them by pressing either the left ("v") or right ("b") response key with their dominant right-hand (right index and middle finger respectively). Each participant completed 702 trials overall split into 9 blocks with short breaks being permitted between blocks. The entire experiment lasted approximately 1 hour.

Experiment 2

Participants performed a forced-choice luminance discrimination task in which they were asked to estimate whether a briefly presented Gaussian patch was lighter or darker than a grey background. On any given trial, the Gaussian patch could take 1 of 3 stimulus intensities corresponding to 25%, 50% and 75% successful detection performance (determined in a previous behavioural titration session). The experiment also included catch trials in which no stimulus was presented. The stimuli were presented using the Psychophysics Toolbox (89, 90) in Matlab (Mathworks, Inc. USA) on a CRT monitor with a 1280 x 1024 pixel resolution and 100 Hz refresh rate at a viewing distance of 57 cm.

Each trial began with presentation of a black fixation cross which remained on the screen for 1.4 s followed by presentation of the dark or light Gaussian patch (0.03 s) in the upper right visual field. The fixation cross was then displayed for 1 sec before a response prompt asked participants to judge whether the stimulus had been lighter (by pressing '1' on the numeric pad of the keyboard with their right hand) or darker (by pressing '2') than the background. After this decision, another response prompt asked participants to rate the clarity of their perception of a four-point scale. Responses were given by pressing four different buttons on the keyboard ('0', '1', '2' and '3' on the numeric pad) and the following trial began immediately after this response. Each participant completed 800 trials overall split into 10 blocks with short breaks being permitted between blocks. The entire experiment lasted approximately 1 hour.

EEG recording and pre-processing

During both experiments, continuous EEG was recorded with two BrainAmp MR Plus units (Brain Products GmbH, Munich, Germany) at a sampling rate of 1000 Hz through 60 (in 16)

and 61 Ag/AgCl pellet pin scalp electrodes (in 48) placed according to the 10-10 International System. Electrode impedance was kept below 10 KΩ. Note that the extra scalp electrode included in (48) was not analysed here in order to equate the montages between the two experiments. Subsequent pre-processing steps for each experiment are described below:

Experiment 1 pre-processing

Pre-processing was performed using a combination of custom scripts incorporating EEGLAB (91) and FieldTrip (92) functions in Matlab (Mathworks, USA). Offline, continuous data were filtered for power line noise using a notch filter centred at 50Hz. Additional low (100 Hz) and high-pass (0.1 Hz) filters were applied using a zero-phase second-order Butterworth filter. The data were then divided into epochs spanning -2.5:1.5 sec relative to stimulus onset on each trial. Subsequently, excessively noisy electrodes were removed without interpolation, the data were re-referenced to the average reference (excluding ocular channels) and trials with abnormal activity were rejected using a semi-automated artefact detection procedure. An independent component analysis (ICA) was then run using the *runica* EEGLAB function (91) and components corresponding to blinks, eye movements and muscle artefacts were removed. Missing channels were then interpolated using a spherical spline method.

Experiment 2 pre-processing

Pre-processing steps were performed using Brain Vision Analyzer 2.0 (BrainProducts). Offline, continuous data were filtered for power line noise using a notch filter centred at 50Hz. Additional low (85 Hz) and high-pass (0.1 Hz) filters were applied using a zero-phase second-order Butterworth filter. ICA was applied to identify and remove eye blinks and muscle artifacts. The data were segmented into epochs of 5 s starting -2.5 sec before stimulus onset

and down sampled to 250 Hz. All epochs were then visually inspected and removed if contaminated by residual eye movements, blinks, strong muscle activity or excessive noise.

Split-half FFT analysis

The artifact-free single-trial data were split into two separate datasets corresponding to the 1st and 2nd halves of the experiment for each participant and re-epoched from -1:0 sec relative to stimulus onset (i.e. 1 sec single-trial baselines). The 1 sec single-trial baselines were then multiplied by a Hamming window, zero padded and fast Fourier transformed in order to retrieve power spectra (frequency resolution = 0.1 Hz) which were averaged over trials separately for the 1st and 2nd half of the experiment. The peak alpha frequency (frequency with highest power between 8-13 Hz) and amplitude were then extracted from the electrode with the highest mean alpha (8-13 Hz) power within each participant separately for each half of the experiment. Paired-samples t-tests were then employed to test for systematic changes in both frequency and power over time. Individual changes in alpha frequency and power were calculated by subtracting the values from the 1st half of the experiment from those in the 2nd. Hence, positive values indicated an increase in frequency/power and negative values indicated a decrease. A Spearman's correlation analysis was performed to assess any relationship between the individual changes in alpha frequency and power over time.

EEG time-frequency transform

Fourier-based spectro-temporal decomposition of the artifact-free single-trial data was performed using the ft_freqanalysis function (frequency-domain wavelet convolution; method: 'mtmconvol') from the FieldTrip toolbox (92), yielding a complex-valued time-frequency plane for each trial. A temporal resolution was maintained by decomposing overlapping 0.5 sec segments of trial time series, consecutively shifted forward in time by 20

ms. Data segments were multiplied with a Hanning taper and then zero-padded to achieve a frequency resolution of 1 Hz across the range of 1:40 Hz. Power values were calculated as the squared absolute values of the complex Fourier Spectra. The data were then re-epoched from -1:1 sec relative to stimulus onset.

Instantaneous alpha frequency (Inst-AF) calculation

The Inst-AF analysis was implemented using methods and code developed by Cohen(46). The single-trial EEG waveforms at all electrodes were filtered between 8 and 13 Hz using a zero-phase (two-pass), plateau-shaped, band-pass filter with 15% transition zones (Matlab *filtfilt* function). Phase angle time series for each electrode were then extracted from the resulting alpha waveforms by means of a Hilbert transform. The instantaneous frequency (in Hz) is defined by the temporal derivative of the phase angle time series (when scaled by the sampling rate and $2\boldsymbol{\pi}$). Noise-induced spikes in the Inst-AF time series were attenuated by application of several median filters of 10 different orders (i.e. corresponding to a minimum of 10 msec and maximum of 400 msec). The median of the resulting values was then taken. The Inst-AF data were then re-epoched from -1:1 sec relative to stimulus onset and averaged over samples in order to match the 20 ms resolution of the time-frequency power.

To test the time-resolved relationship between Inst-AF and power, each variable was z-transformed across all data points (20 ms resolution), trial baselines and electrodes within each participant. The inverted u-shape relationship was formally tested using the two-line solution (49) which involves performing linear regression between the variables separately for 'high' (z-values above 0 collapsed across all samples (electrodes, trials, time points)) and low (z-values below 0) values of the x-axis variable (Inst-AF values). If a significant u-shaped relationship exists, then the coefficients for the 'high' and 'low' regressions should be of

opposite sign and both individually significant. To test an additional influence of time-on-task on the relationship between Inst-AF and power, the data for each variable were also averaged over samples in each single-trial baseline and these baseline-averaged values were also z-transformed across all trials and electrodes within each participant. We tested for both monotonic and inverted u-shaped relationships by means of an overall linear regression between baseline-averaged Inst-AF and power (monotonic) and the two-line solution described above (u-shaped).

Single-trial time-on-task analysis of both time-resolved Inst-AF and alpha-power

Within participant, single-trial correlations were calculated between trial order (1:*N trials*) and each EEG measure separately (Inst-AF and alpha-power) for all electrodes and time-points across the epoch (-1:1 sec relative to stimulus onset, 20 ms resolution) using a two-tailed Spearman's rank analysis. If at a given data-point (electrode/time), the value of the EEG measure systematically changes over time then the Spearman's rho values should show a consistent directionality across participants. Alternatively, if the EEG measure remains relatively stationary or fluctuates spontaneously across trials, then rho values across participants should be random (centred around 0). Hence, for both Inst-AF and alpha-power we performed one-sample t-tests (test against 0) on the Spearman's rho values across participants at all data points (i.e. all electrodes and time points). In order to control the familywise error rate (FWER) across the large number of comparisons, cluster-based permutation testing (50) was employed. Based on the initial one-sample t-tests, all t-values above a threshold corresponding to an uncorrected p-value of 0.05 were formed into clusters by grouping together adjacent significant time-points and electrodes. This step was performed separately for samples with positive and negative t-values (two-tailed test). Note

that for a significant sample to be included in a cluster it was required to have at least 1 adjacent neighbouring significant sample in both space (electrodes) and time**.** The spatial neighbourhood of each electrode was defined as all electrodes within approximately 5 cm, resulting in a mean of 6.3 (min = 3, max = 8) and median of 7 neighbours per electrode. The t-values within each cluster were then summed to produce a cluster statistic. Subsequently, this procedure was repeated across 2000 permutations to create a data-driven null hypothesis distribution using *ft_statistics_montecarlo* (92) . On each iteration, this function effectively switched the sign of the correlation for a random subset of the participants. One-sample t-tests of rho values against zero were then performed at each data point. After clustering significant t-values across neighbouring data points (as above), the most extreme cluster-level t-score was retained. The location of the original real cluster statistics within this null hypothesis distribution indicates how probable such observations would be if the null hypothesis were true. Hence, if a given negative/positive cluster had a cluster statistic lower/higher than 97.5% of the respective null distribution cluster statistics, then this was considered a significant effect (5% alpha level).

Split-half stratification FFT analysis

Single-trial values of both alpha power (8:13 Hz) and Inst-AF were averaged over the baseline period (-1:0 sec) across all electrodes and the data were split into bins corresponding to the 1st and 2nd half of the experiment in each participant. The mean, variance and higher order statistics of both the 1st and 2nd half trial distributions of one of the measures (either alpha-power or Inst-AF) were equalized by sub-sampling the single trials using the *ft_stratify* function ('histogram' method with 100 bins) in FieldTrip (92). The stratification was performed separately for alpha power and frequency. Because the stratification algorithm

approximately equalizes the trial distributions and the results are not necessarily identical each time it is run, the peak alpha frequency and amplitude were extracted from the electrode with the highest mean alpha (8-13 Hz) amplitude (using the same FFT analysis as described above across the trials remaining after stratification) on every iteration of 100 runs of the analysis and averaged (separately for the 1st and 2nd half distributions) within each participant. On average, 211 trials (min = 141, max = 320) remained in each distribution after stratification of alpha power and 190 trials (min = 108, max = 267) remained after stratification of alpha-frequency. The peak alpha frequency and power values were entered into paired-samples t-tests to test for systematic changes in either frequency or power over time after approximate equalisation of the other variable.

Acknowledgements

We would like to thank Dr. Mike X. Cohen for EEG analysis scripts and useful discussions regarding interpretation. This work was supported by grants from the Wellcome Trust (grant numbers 098434 and 098433 to GT and JG respectively) and the UK Economic and Social Research Council (grant number ES/I02395X/1 to CSYB).

Conflict of Interest The authors declare no conflict of interest.

References

1. Buzsáki G, Logothetis N, & Singer W (2013) Scaling Brain Size, Keeping Timing: Evolutionary Preservation of Brain Rhythms. *Neuron* 80(3):751-764.
2. Berger H (1929) Über das Elektrenkephalogramm des Menschen. *Archiv für Psychiatrie und Nervenkrankheiten* 87(1):527-570.
3. Ward LM (2003) Synchronous neural oscillations and cognitive processes. *Trends in Cognitive Sciences* 7(12):553-559.
4. Kahana MJ (2006) The Cognitive Correlates of Human Brain Oscillations. *Journal of Neuroscience* 26(6):1669-1672.

5. Varela F, Lachaux J-P, Rodriguez E, & Martinerie J (2001) *Nature Reviews Neuroscience* 2(4):229-239.
6. Salinas E & Sejnowski TJ (2001) Correlated neuronal activity and the flow of neural information. *Nature Reviews Neuroscience* 2(8):539-550.
7. Fries P (2005) A mechanism for cognitive dynamics: neuronal communication through neuronal coherence. *Trends in Cognitive Sciences* 9(10):474-480.
8. Schyns PG, Thut G, & Gross J (2011) Cracking the Code of Oscillatory Activity. *PLoS Biology* 9(5):e1001064.
9. Siegel M, Donner TH, & Engel AK (2012) Spectral fingerprints of large-scale neuronal interactions. *Nature Reviews Neuroscience*.
10. Fries P (2015) Rhythms for Cognition: Communication through Coherence. *Neuron* 88(1):220-235.
11. Bonnefond M, Kastner S, & Jensen O (2017) Communication between Brain Areas Based on Nested Oscillations. *eneuro* 4(2):ENEURO.0153-0116.2017.
12. van Dijk H, Schoffelen JM, Oostenveld R, & Jensen O (2008) Prestimulus Oscillatory Activity in the Alpha Band Predicts Visual Discrimination Ability. *Journal of Neuroscience* 28(8):1816-1823.
13. Chaumon M & Busch NA (2014) Prestimulus Neural Oscillations Inhibit Visual Perception via Modulation of Response Gain. *Journal of Cognitive Neuroscience* 26(11):2514-2529.
14. VanRullen R (2016) Perceptual Cycles. *Trends in Cognitive Sciences* 20(10):723-735.
15. Iemi L, Chaumon M, Crouzet SM, & Busch NA (2017) Spontaneous Neural Oscillations Bias Perception by Modulating Baseline Excitability. *The Journal of Neuroscience* 37(4):807-819.
16. Benwell CSY*, et al.* (2017) Prestimulus EEG Power Predicts Conscious Awareness But Not Objective Visual Performance. *eneuro* 4(6):ENEURO.0182-0117.2017.
17. Worden MS, Foxe JJ, Wang N, & Simpson GV (2000) Anticipatory biasing of visuospatial attention indexed by retinotopically specific alpha-band electroencephalography increases over occipital cortex. *J Neurosci* 20(6):RC63.
18. Thut G, Nietzel A, Brandt SA, & Pascual-Leone A (2006) Alpha-band electroencephalographic activity over occipital cortex indexes visuospatial attention bias and predicts visual target detection. *J Neurosci* 26(37):9494-9502.
19. Foxe JJ & Snyder AC (2011) The Role of Alpha-Band Brain Oscillations as a Sensory Suppression Mechanism during Selective Attention. *Frontiers in Psychology* 2.
20. Klimesch W (1999) EEG alpha and theta oscillations reflect cognitive and memory performance: a review and analysis. *Brain Research Reviews* 29(2-3):169-195.
21. Jokisch D & Jensen O (2007) Modulation of Gamma and Alpha Activity during a Working Memory Task Engaging the Dorsal or Ventral Stream. *Journal of Neuroscience* 27(12):3244-3251.
22. Klimesch W (2012) Alpha-band oscillations, attention, and controlled access to stored information. *Trends in Cognitive Sciences* 16(12):606-617.
23. Bonnefond M & Jensen O (2012) Alpha Oscillations Serve to Protect Working Memory Maintenance against Anticipated Distracters. *Current Biology* 22(20):1969-1974.
24. Romei V*, et al.* (2007) Spontaneous Fluctuations in Posterior -Band EEG Activity Reflect Variability in Excitability of Human Visual Areas. *Cerebral Cortex* 18(9):2010-2018.
25. Haegens S, Nacher V, Luna R, Romo R, & Jensen O (2011) Alpha-Oscillations in the monkey sensorimotor network influence discrimination performance by rhythmical inhibition of neuronal spiking. *Proceedings of the National Academy of Sciences* 108(48):19377-19382.
26. Lange J, Oostenveld R, & Fries P (2013) Reduced Occipital Alpha Power Indexes Enhanced Excitability Rather than Improved Visual Perception. *Journal of Neuroscience* 33(7):3212-3220.
27. Klimesch W, Sauseng P, & Hanslmayr S (2007) EEG alpha oscillations: The inhibition–timing hypothesis. *Brain Research Reviews* 53(1):63-88.

28. Jensen O & Mazaheri A (2010) Shaping Functional Architecture by Oscillatory Alpha Activity: Gating by Inhibition. *Frontiers in Human Neuroscience* 4.
29. Zumer JM, Scheeringa R, Schoffelen J-M, Norris DG, & Jensen O (2014) Occipital Alpha Activity during Stimulus Processing Gates the Information Flow to Object-Selective Cortex. *PLoS Biology* 12(10):e1001965.
30. Hughes SW & Crunelli V (2005) Thalamic Mechanisms of EEG Alpha Rhythms and Their Pathological Implications. *The Neuroscientist* 11(4):357-372.
31. Bollimunta A, Mo J, Schroeder CE, & Ding M (2011) Neuronal Mechanisms and Attentional Modulation of Corticothalamic Alpha Oscillations. *Journal of Neuroscience* 31(13):4935-4943.
32. Haegens S*, et al.* (2015) Laminar Profile and Physiology of the Rhythm in Primary Visual, Auditory, and Somatosensory Regions of Neocortex. *Journal of Neuroscience* 35(42):14341-14352.
33. Scheeringa R, Koopmans PJ, van Mourik T, Jensen O, & Norris DG (2016) The relationship between oscillatory EEG activity and the laminar-specific BOLD signal. *Proceedings of the National Academy of Sciences* 113(24):6761-6766.
34. Keitel A & Gross J (2016) Individual Human Brain Areas Can Be Identified from Their Characteristic Spectral Activation Fingerprints. *PLOS Biology* 14(6):e1002498.
35. Barzegaran E, Vildavski VY, & Knyazeva MG (2017) Fine Structure of Posterior Alpha Rhythm in Human EEG: Frequency Components, Their Cortical Sources, and Temporal Behavior. *Scientific Reports* 7(1).
36. Clayton MS, Yeung N, & Cohen Kadosh R (2017) The many characters of visual alpha oscillations. *Eur J Neurosci*.
37. Gross J (2014) Analytical methods and experimental approaches for electrophysiological studies of brain oscillations. *Journal of Neuroscience Methods* 228:57-66.
38. Cohen MX (2017) Where Does EEG Come From and What Does It Mean? *Trends in Neurosciences* 40(4):208-218.
39. Cole SR & Voytek B (2017) Brain Oscillations and the Importance of Waveform Shape. *Trends in Cognitive Sciences* 21(2):137-149.
40. Cole SR*, et al.* (2017) Nonsinusoidal Beta Oscillations Reflect Cortical Pathophysiology in Parkinson's Disease. *The Journal of Neuroscience* 37(18):4830-4840.
41. Jones SR (2016) When brain rhythms aren't 'rhythmic': implication for their mechanisms and meaning. *Current Opinion in Neurobiology* 40:72-80.
42. Simon M*, et al.* (2011) EEG alpha spindle measures as indicators of driver fatigue under real traffic conditions. *Clinical Neurophysiology* 122(6):1168-1178.
43. Mathewson KJ*, et al.* (2015) Regional electroencephalogram (EEG) alpha power and asymmetry in older adults: a study of short-term test–retest reliability. *Frontiers in Aging Neuroscience* 7.
44. Kasten FH, Dowsett J, & Herrmann CS (2016) Sustained Aftereffect of α-tACS Lasts Up to 70 min after Stimulation. *Frontiers in Human Neuroscience* 10.
45. Haegens S, Cousijn H, Wallis G, Harrison PJ, & Nobre AC (2014) Inter- and intra-individual variability in alpha peak frequency. *NeuroImage* 92:46-55.
46. Cohen MX (2014) Fluctuations in Oscillation Frequency Control Spike Timing and Coordinate Neural Networks. *Journal of Neuroscience* 34(27):8988-8998.
47. Mierau A, Klimesch W, & Lefebvre J (2017) State-dependent alpha peak frequency shifts: Experimental evidence, potential mechanisms and functional implications. *Neuroscience* 360:146-154.
48. Benwell CSY, Keitel C, Harvey M, Gross J, & Thut G (2017) Trial-by-trial co-variation of pre-stimulus EEG alpha power and visuospatial bias reflects a mixture of stochastic and deterministic effects. *European Journal of Neuroscience*.
49. Simonsohn U (2017) Two-Lines: A valid Alternative to the Invalid Testing of U-Shaped Relationships with Quadratic Regressions. *SSRN Electronic Journal*.

50. Maris E & Oostenveld R (2007) Nonparametric statistical testing of EEG- and MEG-data. *Journal of Neuroscience Methods* 164(1):177-190.
51. Pfurtscheller G, Stancák A, & Neuper C (1996) Event-related synchronization (ERS) in the alpha band — an electrophysiological correlate of cortical idling: A review. *International Journal of Psychophysiology* 24(1-2):39-46.
52. Rihs TA, Michel CM, & Thut G (2007) Mechanisms of selective inhibition in visual spatial attention are indexed by ?-band EEG synchronization. *European Journal of Neuroscience* 25(2):603-610.
53. Palva S & Palva JM (2007) New vistas for α-frequency band oscillations. *Trends in Neurosciences* 30(4):150-158.
54. Boksem MA, Meijman TF, & Lorist MM (2005) Effects of mental fatigue on attention: an ERP study. *Brain Res Cogn Brain Res* 25(1):107-116.
55. Cajochen C, Brunner DP, Krauchi K, Graw P, & Wirz-Justice A (1995) Power Density in Theta/Alpha Frequencies of the Waking EEG Progressively Increases During Sustained Wakefulness. *Sleep* 18(10):890-894.
56. Craig A, Tran Y, Wijesuriya N, & Nguyen H (2012) Regional brain wave activity changes associated with fatigue. *Psychophysiology* 49(4):574-582.
57. Bompas A, Sumner P, Muthumumaraswamy SD, Singh KD, & Gilchrist ID (2015) The contribution of pre-stimulus neural oscillatory activity to spontaneous response time variability. *NeuroImage* 107:34-45.
58. Benwell CSY, Harvey M, Gardner S, & Thut G (2013) Stimulus- and state-dependence of systematic bias in spatial attention: Additive effects of stimulus-size and time-on-task. *Cortex* 49(3):827-836.
59. Aurlien H*, et al.* (2004) EEG background activity described by a large computerized database. *Clinical Neurophysiology* 115(3):665-673.
60. Nir R-R, Sinai A, Raz E, Sprecher E, & Yarnitsky D (2010) Pain assessment by continuous EEG: Association between subjective perception of tonic pain and peak frequency of alpha oscillations during stimulation and at rest. *Brain Research* 1344:77-86.
61. Maurer U*, et al.* (2014) Frontal Midline Theta Reflects Individual Task Performance in a Working Memory Task. *Brain Topography* 28(1):127-134.
62. Hülsdünker T, Mierau A, & Strüder HK (2016) Higher Balance Task Demands are Associated with an Increase in Individual Alpha Peak Frequency. *Frontiers in Human Neuroscience* 9.
63. Buzsaki G (2004) Neuronal Oscillations in Cortical Networks. *Science* 304(5679):1926-1929.
64. Laufs H*, et al.* (2003) EEG-correlated fMRI of human alpha activity. *NeuroImage* 19(4):1463-1476.
65. Magri C, Schridde U, Murayama Y, Panzeri S, & Logothetis NK (2012) The Amplitude and Timing of the BOLD Signal Reflects the Relationship between Local Field Potential Power at Different Frequencies. *Journal of Neuroscience* 32(4):1395-1407.
66. Bollimunta A, Chen Y, Schroeder CE, & Ding M (2008) Neuronal Mechanisms of Cortical Alpha Oscillations in Awake-Behaving Macaques. *Journal of Neuroscience* 28(40):9976-9988.
67. Sadaghiani S*, et al.* (2010) Intrinsic Connectivity Networks, Alpha Oscillations, and Tonic Alertness: A Simultaneous Electroencephalography/Functional Magnetic Resonance Imaging Study. *Journal of Neuroscience* 30(30):10243-10250.
68. Buffalo EA, Fries P, Landman R, Buschman TJ, & Desimone R (2011) Laminar differences in gamma and alpha coherence in the ventral stream. *Proceedings of the National Academy of Sciences* 108(27):11262-11267.
69. Mo J, Schroeder CE, & Ding M (2011) Attentional Modulation of Alpha Oscillations in Macaque Inferotemporal Cortex. *Journal of Neuroscience* 31(3):878-882.
70. Capilla A, Schoffelen J-M, Paterson G, Thut G, & Gross J (2012) Dissociated α-Band Modulations in the Dorsal and Ventral Visual Pathways in Visuospatial Attention and Perception. *Cerebral Cortex* 24(2):550-561.

71. Caspers H (1983) Electroencephalography: Basic Principles, Clinical Applications and Related Fields. Ernst Niedermeyer , Fernando Lopes da Silva. *The Quarterly Review of Biology* 58(2):301-302.
72. Meisen P (2016) TIDAMODEL: Modeling Time Interval Data. in *Analyzing Time Interval Data* (Springer Fachmedien Wiesbaden), pp 73-89.
73. Frund I, Haenel NV, & Wichmann FA (2011) Inference for psychometric functions in the presence of nonstationary behavior. *Journal of Vision* 11(6):16-16.
74. Doll RJ, Veltink PH, & Buitenweg JR (2015) Observation of time-dependent psychophysical functions and accounting for threshold drifts. *Attention, Perception, & Psychophysics* 77(4):1440-1447.
75. Gulbinaite R, van Viegen T, Wieling M, Cohen MX, & VanRullen R (2017) Individual alpha peak frequency predicts 10 Hz flicker effects on selective attention. (Cold Spring Harbor Laboratory).
76. Notbohm A & Herrmann CS (2016) Flicker Regularity Is Crucial for Entrainment of Alpha Oscillations. *Frontiers in Human Neuroscience* 10.
77. Spaak E, de Lange FP, & Jensen O (2014) Local Entrainment of Alpha Oscillations by Visual Stimuli Causes Cyclic Modulation of Perception. *Journal of Neuroscience* 34(10):3536-3544.
78. Mathewson KE*, et al.* (2012) Making Waves in the Stream of Consciousness: Entraining Oscillations in EEG Alpha and Fluctuations in Visual Awareness with Rhythmic Visual Stimulation. *Journal of Cognitive Neuroscience* 24(12):2321-2333.
79. de Graaf TA*, et al.* (2013) Alpha-Band Rhythms in Visual Task Performance: Phase-Locking by Rhythmic Sensory Stimulation. *PLoS ONE* 8(3):e60035.
80. Capilla A, Pazo-Alvarez P, Darriba A, Campo P, & Gross J (2011) Steady-state visual evoked potentials can be explained by temporal superposition of transient event-related responses. *PLoS One* 6(1):e14543.
81. Keitel C, Quigley C, & Ruhnau P (2014) Stimulus-Driven Brain Oscillations in the Alpha Range: Entrainment of Intrinsic Rhythms or Frequency-Following Response? *Journal of Neuroscience* 34(31):10137-10140.
82. Romei V, Thut G, & Silvanto J (2016) Information-Based Approaches of Noninvasive Transcranial Brain Stimulation. *Trends in Neurosciences* 39(11):782-795.
83. Thut G*, et al.* (2017) Guiding transcranial brain stimulation by EEG/MEG to interact with ongoing brain activity and associated functions: A position paper. *Clinical Neurophysiology* 128(5):843-857.
84. Klimesch W, Sauseng P, & Gerloff C (2003) Enhancing cognitive performance with repetitive transcranial magnetic stimulation at human individual alpha frequency. *European Journal of Neuroscience* 17(5):1129-1133.
85. Helfrich Randolph F*, et al.* (2014) Entrainment of Brain Oscillations by Transcranial Alternating Current Stimulation. *Current Biology* 24(3):333-339.
86. Samaha J & Postle Bradley R (2015) The Speed of Alpha-Band Oscillations Predicts the Temporal Resolution of Visual Perception. *Current Biology* 25(22):2985-2990.
87. Cecere R, Rees G, & Romei V (2015) Individual Differences in Alpha Frequency Drive Crossmodal Illusory Perception. *Current Biology* 25(2):231-235.
88. Schneider W, Eschman A, & Zuccolotto A (2002) E-Prime User's Guide (Psychology Software Tools Inc, Pittsburgh, PA).
89. Brainard DH (1997) The Psychophysics Toolbox. *Spatial Vision* 10(4):433-436.
90. Pelli DG (1997) The VideoToolbox software for visual psychophysics: transforming numbers into movies. *Spatial Vision* 10(4):437-442.
91. Delorme A & Makeig S (2004) EEGLAB: an open source toolbox for analysis of single-trial EEG dynamics including independent component analysis. *Journal of Neuroscience Methods* 134(1):9-21.

92. Oostenveld R, Fries P, Maris E, & Schoffelen J-M (2011) FieldTrip: Open Source Software for Advanced Analysis of MEG, EEG, and Invasive Electrophysiological Data. *Computational Intelligence and Neuroscience* 2011:1-9.